

# New transient Galactic bulge intermediate polar candidate XMMU J175035.2-293557

F. Hofmann<sup>1</sup>, G. Ponti<sup>1</sup>, F. Haberl<sup>1</sup>, and M. Clavel<sup>2</sup>

<sup>1</sup> Max-Planck-Institut für extraterrestrische Physik, Giessenbachstraße, 85748 Garching, Germany

<sup>2</sup> Univ. Grenoble Alpes, CNRS, Institut de Planétologie et d'Astrophysique de Grenoble (IPAG), 38000, Grenoble, France

Received ..., accepted ...

## ABSTRACT

**Context.** For the past decades a rare subclass of cataclysmic variables (CV), with magnetized white dwarfs (WD) as accretors has been studied and called intermediate polars (IP). They have been discussed as the main contributor to the diffuse X-ray emission due to unresolved point sources close to the Galactic center (GC) and in the Galactic bulge (GB).

**Aims.** In an ongoing X-ray survey (0.5-10 keV energy band) of  $3^\circ \times 3^\circ$  around the GC with the *XMM-Newton* observatory we conducted a systematic search for transient X-ray sources.

**Methods.** Promising systems were analyzed for spectral, timing, and multi-wavelength properties to constrain their nature.

**Results.** We discovered a new highly variable (factor  $\geq 20$ ) X-ray source about  $1.25^\circ$  south of the GC. We found evidence making the newly discovered system a candidate IP. The X-ray light curve shows a period of  $511 \pm 10$  s which can be interpreted as the spin period of the WD. The X-ray spectrum is well fit by a bremsstrahlung model with a temperature of  $13.9 \pm 2.5$  keV, suggesting a WD mass of  $0.4 - 0.5 M_\odot$ . Among many candidates we could not identify a blue optical counterpart as would be expected for IPs.

**Conclusions.** The high X-ray absorption and absence of a clear optical counterpart suggest that the source is most likely located in the GB. This would make the system a transient IP (GK Per class) with especially high peak X-ray luminosity and therefore a very faint X-ray transient (VFXT).

**Key words.** X-ray: binaries; Galaxy: center; Galaxy: bulge; white dwarfs; cataclysmic variables

## 1. Introduction

Intermediate polars (IP) are a subclass of magnetic cataclysmic variables (CV) where a white dwarf (WD) is accreting mass from a late-type donor star (see e.g. Downes et al. 2001; Mukai 2017). The accretion disk around the WD is interrupted by the magnetic field and matter is accreted along the field lines onto the magnetic poles of the WD. X-ray emission is created in accretion curtains onto the magnetic poles and the accretion disk of the WD (e.g. Patterson 1994; Hellier 2007; Barbera et al. 2017). IPs usually show light curve modulations (X-ray and optical) by the spin of the WD and the orbital period around its donor star (see e.g. Watson et al. 1985; Osborne 1988; Cropper 1990; Kim & Beuermann 1995). There are about 50 confirmed IPs and more than 100 candidates known today (see IP catalogue maintained by Koji Mukai<sup>1</sup>).

Recently IPs have been discussed as the origin of the hard ( $\sim 2 - 40$  keV range) X-ray emission close to the Galactic center (GC) and in the Galactic bulge (GB) region (e.g. Krivonos et al. 2007; Revnivtsev et al. 2009; Perez et al. 2015; Hailey et al. 2016). Pretorius & Mukai (2014) estimated the space density of IPs from a *Swift*-BAT survey (14-195 keV), where due to their high temperature X-ray spectrum, they are brighter than in the 0.5-10 keV band. Munro et al. (2004), Laycock et al. (2005), and Ruiters et al. (2006) derived from a deep *Chandra* survey that most fainter, hard GC X-ray sources should be IPs. Investigating the population of IPs in the GB/GC area is therefore very important for understanding their contribution to the diffuse X-ray emission (Hong 2012). In addition IPs trace the CV popu-

lation (see Cropper 1990) which is important to understand the GB stellar composition (e.g. Calamida et al. 2014, 2015).

Because IPs are relatively faint in X-rays and optical and due to high extinction towards the GC, deep and high spatial resolution observations are needed. We used the extension of the deep *XMM-Newton* GC X-ray survey (about 0.5-10 keV energy band, Ponti et al. 2015) to the GB (Ponti et al., in prep.) to search for transients and highly variable sources (overall  $\sim 3^\circ \times 3^\circ$ ). We detected a new X-ray source  $1.25^\circ$  south of Sgr A\* (in Galactic coordinates). The analysis of the X-ray spectrum, search for periodic modulations and lack optical counterpart identification make the source an IP candidate most likely located in the GB, which are rarely observed (see Hong et al. 2009; Britt et al. 2013; Torres et al. 2014; Johnson et al. 2017). A larger sample of clearly identified IPs in the GB will be needed for direct population constraints. As a luminous, transient IP, the source would be the second member of the GK Per class (see recent description by Yuasa et al. 2016), and might have a subgiant donor star.

## 2. X-ray data

The analysis in this work is based on a 25 ks *XMM-Newton* observation (ObsID: 0801681401, start date 2017-10-07, PI: Ponti). We used data from the *XMM-Newton* European Photon Imaging Camera (EPIC) PN (Strüder et al. 2001), and MOS CCDs (Turner et al. 2001). The spectral fitting was performed using XSPEC (version 12.9.1n, Arnaud 1996) and the Bayesian fitting package BXA (Buchner et al. 2014). The data reduction was performed using the *XMM-Newton* Science Analysis System (SAS) version 16.1.0. Long-term source variability in-

<sup>1</sup> <https://asd.gsfc.nasa.gov/Koji.Mukai/iphome/>

formation was obtained together with previous 15 ks and 2 ks *Chandra* (description see Garmire et al. 2003) observations (ObsIDs: 7167, start date 2006-10-30, PI: Grindlay; 8753, start date 2008-05-13, PI: Jonker), which were part of the *Chandra* Galactic bulge survey (Jonker et al. 2011). These observations were reprocessed using the *Chandra* Interactive Analysis of Observations software package (CIAO; Fruscione et al. 2006) version 4.5 and the *Chandra* Calibration Database (CalDB; Graessle et al. 2007) version 4.5.9. Uncertainties are quoted on the  $1\sigma$  level unless stated otherwise.

### 3. Results

The source position is R.A.:  $17^{\text{h}}50^{\text{m}}35^{\text{s}}.2$  Dec.:  $-29^{\circ}35'57''.2$  with an uncertainty of  $1.2''$  (systematic, see *XMM-Newton* technical note: XMM-SOC-CAL-TN-0018) plus  $0.5''$  (statistical), leading to  $1.3''$  total  $1\sigma$  uncertainty. A cross correlation of detected sources in the *XMM-Newton* observation with the *Chandra* Galactic Bulge survey catalogue of X-ray and optical sources (Jonker et al. 2014; Wevers et al. 2016) showed an average offset of less than  $1''$  in both R.A. and Dec. direction.

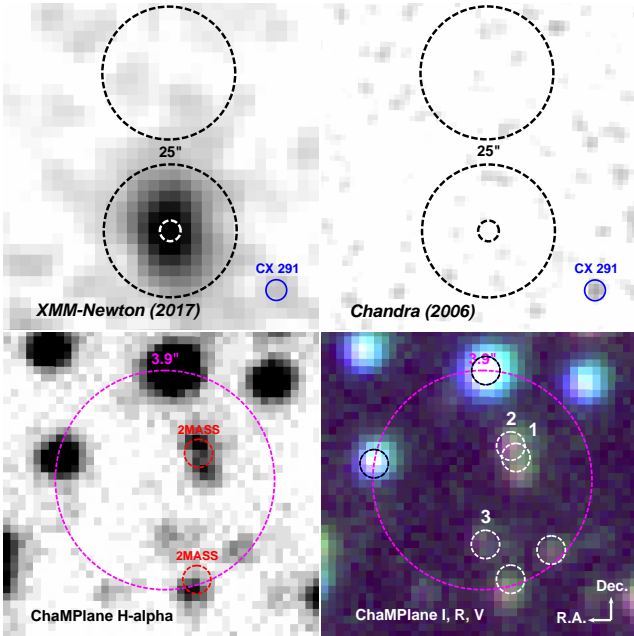


**Fig. 1.** **Top left:** *XMM-Newton* EPIC 1-2 keV flux image (from 2017-10-07,  $4 \times 4''$  pixel size, smoothed by a 2 pixel Gaussian). Circular extraction regions ( $25''$  radius) of source and background counts (black dashed),  $3\sigma$  positional uncertainty (white dashed). **Top right:** *Chandra* ACIS-I 1-2 keV flux image (from 2006-10-30,  $2 \times 2''$  pixel size, smoothed by a 2 pixel Gaussian). The blue circle indicates a source from the Jonker et al. (2014) *Chandra* catalogue. **Bottom left:** Zoomed ChaMPPlane (Grindlay et al. 2003)  $H\alpha$  image (red circles: 2MASS sources, magenta circle:  $3\sigma$  X-ray positional uncertainty). **Bottom right:** ChaMPPlane colour band image (red: I, green: R, blue: V). Small circles are correlated sources from Wevers et al. (2016) with the three closest numbered.

#### 3.1. X-ray spectrum and variability

We extracted the source and background spectra (0.5-10 keV) from two  $25''$  radius circles shown in Fig. 1, using standard event file filtering and grouped the spectrum to contain at least 22 counts per bin. The background region was chosen to con-

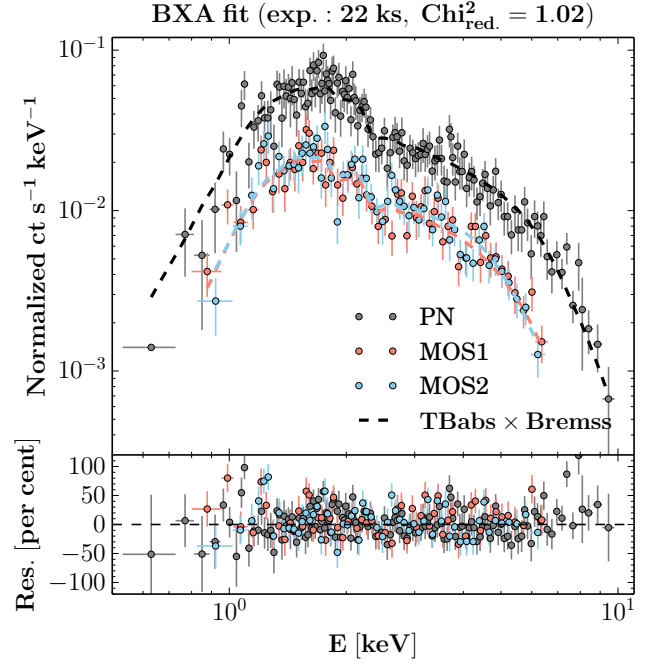


**Fig. 2.** *XMM-Newton* EPIC spectrum (0.5-10 keV) for PN, MOS1, and MOS2 separately with residuals of a TBabs $\times$ brems model fitted using BXA in pyXSPEC.

**Table 1.** *XMM-Newton* spectral model parameters (0.5-10 keV range).

	pow <sup>a</sup>	diskbb <sup>a</sup>	brems <sup>a</sup>	apec <sup>a, c</sup>
$N_{\text{H}}^b$	$3.6 \pm 0.2$	$1.0 \pm 0.1$	$1.2 \pm 0.1$	$1.3 \pm 0.1$
$kT^b$	-	$2.2 \pm 0.1$	$13.9 \pm 2.5$	$15.5 \pm 2.5$
$\Gamma^b$	2.8	-	-	-
$F_{\text{X}}^b$	1.6	1.7	1.7	1.7
$\chi^2/\text{dof}^b$	619/260	302/260	265/260	273/258

**Notes.** <sup>(a)</sup> Implemented with BXA fitting in pyXSPEC. <sup>(b)</sup> Hydrogen column density  $N_{\text{H}}$  [ $10^{22} \text{ cm}^{-2}$ ], temperature  $kT$  [keV], power law photon index  $\Gamma$ , X-ray flux  $F_{\text{X}}$  (0.5 – 10 keV)  $10^{-12} \text{ erg s}^{-1} \text{ cm}^{-2}$  (uncertainties  $\sim 3 \times 10^{-14} \text{ erg s}^{-1} \text{ cm}^{-2}$ ), and goodness of fit ( $\chi^2$ ) with degrees of freedom (dof) in the fit. <sup>(c)</sup> metal abundance fixed to solar.

tain the same level of enhanced X-ray emission as the source region (caused by extended recombining plasma south of the GC, see Nakashima et al. 2013). The *XMM-Newton* EPIC spectrum contains  $\sim 6 \times 10^3$  net counts (0.5-10 keV range). Table 1 shows the best fit parameters and goodness of fit ( $\chi^2$ ) for several absorbed single-component spectral models. The fitted parameters were obtained using the BXA fitting software with wide and flat priors. For every tested parameter combination the model flux was calculated. The lower limit, best fit value, and upper limit are the 15, 50, and 85 percentiles of the parameter distributions (transformed into symmetric uncertainties). The analysis shows that bremsstrahlung (brems) is the best fitting model compared to a disk-blackbody (diskbb,  $\Delta\chi^2 = 37$ ) or powerlaw (pow,  $\Delta\chi^2 = 354$ ). A collisionally ionized plasma (apec) model with solar abundance would also fit the data well (see Table 1). There is no evidence for an Fe-line complex in the 6 – 7 keV range. We obtained  $3\sigma$  upper limits on the equivalent width (EW) of emission lines

at energies:  $\text{EW}(6.4 \text{ keV}) \lesssim 400 \text{ eV}$ ,  $\text{EW}(6.7 \text{ keV}) \lesssim 220 \text{ eV}$ , and  $\text{EW}(7.0 \text{ keV}) \lesssim 450 \text{ eV}$  (main peaks of the Fe-line complex, see e.g. Hellier & Mukai 2004) by adding additional narrow Gaussian lines to the brems model. The measured foreground column density of neutral hydrogen was fitted as  $N_{\text{H}} \approx (1.2 \pm 0.1) \times 10^{22} \text{ cm}^{-2}$  using the TBabs model with cross-sections and abundances from Wilms et al. (2000).

Using the best fit TBabs  $\times$  brems model the *XMM-Newton* count rate of  $\sim 0.3 \text{ ct s}^{-1}$  translates into a flux of  $1.7 \times 10^{-12} \text{ erg s}^{-1} \text{ cm}^{-2}$  (here 0.5–7.0 keV, for comparison with *Chandra*). The  $3\sigma$  upper limit from previous *Chandra* observations of  $\sim 0.005 \text{ ct s}^{-1}$  translates to  $8.6 \times 10^{-14} \text{ erg s}^{-1} \text{ cm}^{-2}$  (0.5–7.0 keV). This means the source flux varies by a factor of  $\gtrsim 20$  on long time scales ( $\sim 10 \text{ yr}$  between upper limit and detection). Within the *XMM-Newton* EPIC PN observation the flux varies significantly ( $\sim 5\sigma$ ) by up to a factor of  $\sim 4$  on time scales of minutes (77 s binning, see Fig. 3). The source is also covered as part of the Swift Galactic bulge survey (Shaw et al. 2017) with the *Neil Gehrels Swift Observatory* X-ray telescope (mission description, see Burrows et al. 2005) in 2017 and 2018, but the 60–120 s exposures did not allow to significantly constrain the long term light curve. Recent Swift ToO observations (ObsIDs: 00010652001/2, 2018-04-08/10) and a renewed coverage within the *XMM-Newton* GC/GB survey (ObsID: 0801682101, 2018-03-18) provide an upper limit of  $F_{\text{X}} \lesssim 7.2 \times 10^{-14} \text{ erg s}^{-1} \text{ cm}^{-2}$  (a factor of  $\gtrsim 20$  fainter again).

### 3.2. X-ray periodicity

We extracted X-ray light curves for source and background from the same regions as the spectra for 24.7 ks of observation with the PN, MOS1, and MOS2 instruments. We used standard event filtering, barycentric photon arrival time corrections, and the same good time intervals (GTI) to obtain background subtracted, vignetted corrected 0.5 – 10 keV light curves from all instruments.

We performed a Lomb-Scargle analysis (Scargle 1982) with the periodogram tool provided by the NASA exoplanet archive<sup>2</sup> and found a peak at  $\sim 511 \text{ s}$  in the unbinned PN data (confirmed by the MOS1 data at lower significance because of its smaller effective area). We discard MOS2 in the following analysis because of higher and less stable background<sup>3</sup>. The period was found independent of the light curve binning.

For a more detailed significance analysis, 77 s binning was chosen as a compromise between time resolution and measurement uncertainty in each bin. Fig. 3 shows the light curve of PN+MOS1 and the power spectral density (PSD) calculated for 161 frequencies (total power:  $1213 \text{ ct}^2 \text{ s}^{-1}$ ) with the Fast Fourier Transform (FFT) periodogram function of the *scipy* Python package (version 0.17.1). To estimate the significance of the 511 s peak we simulated  $10^6$  light curves with root mean square (RMS) amplitude normalized to the measured signal. White noise simulations best reproduced the observed PSD, leading to the flat significance contours seen in Fig. 3. The most significant peak is located at  $511 \pm 10 \text{ s}$  ( $\sim 3.7\sigma$ ), consistent with the independent Lomb-Scargle analysis (see above). In addition we performed simulations with a pink to red noise PSD, breaking at a period of 500 s (typical for CVs, e.g. Dobrotka et al. 2014). The

results indicate that even in this case the periodicity is significant at  $\sim 3.9\sigma$ .

Fig. 4 shows the PN light curve folded by a 511 s period. The resulting phase diagram is best fit by a sine function with amplitude  $0.17 \pm 0.02$  (translating into  $\sim 17$  per cent pulsed fraction). The fit to a constant value results in  $\chi^2/\text{dof} \approx 39.2/6$  which is further evidence for variability with the folded period.

### 3.3. Correlation with optical sources

The simultaneous *XMM-Newton* optical monitor observation could not be used for counterpart constraints, because the source was outside its field of view. The closest correlation at  $\sim 1.5''$  ( $\sim 1\sigma$  uncertainty) of the X-ray position is 2MASS 17503510-2935562 (Cutri et al. 2003) with  $\sim 13 \text{ (J,H,K)}_{\text{mag}}$  (Fig. 1, bottom left). The Yale/San Juan Southern Proper Motion Catalog (Girard et al. 2011) provides a proper motion of  $\sim 80 \text{ mas/yr}$  for the 2MASS source, which would make it most likely a foreground M star. The VISTA Variable in the Via Lactea Survey DR2 (Minniti et al. 2017) provides  $\sim 16, 15, 14, 13 \text{ (Z,Y,J,H)}_{\text{mag}}$  for the position.

The 2MASS position is resolved into two optical sources in the *Chandra* Galactic Bulge survey (Wevers et al. 2016), and the OGLEII survey (Udalski et al. 2002) - both  $\sim 21, 17 \text{ (V,I)}_{\text{mag}}$  (sources 1 and 2, Fig. 1, bottom). The OGLEII light curves (about one observation per day) of possible counterparts show no significant variability, but because of relatively large uncertainties this does not exclude intrinsic variability.

The Gaia DR2 catalogue (Gaia Collaboration et al. 2018) constrains the distance to source 1 (Fig. 1, bottom) to  $\sim 0.8 - 2.2 \text{ kpc}$ , and source 2 to  $\gtrsim 1.4 \text{ kpc}$ , with proper motions of 14 and 11 mas/yr respectively, and both  $G_{\text{mag}} \sim 19$ .

## 4. Discussion

In the *XMM-Newton* GC/GB scan of currently  $\sim 6 \text{ deg}^2$ , XMMU J175035.2-293557 is a rare intermediate brightness, hard, and strongly variable X-ray source.

### 4.1. IP properties from X-rays

A bremsstrahlung model being the best fit to the X-ray spectrum and the evidence for a 511 s period are strong indications that the source is an IP. The best fit temperature of a brems model is  $13.9 \pm 2.5 \text{ keV}$  which would suggest a WD mass of about  $0.4 - 0.5 M_{\odot}$  (at the low end of the known mass function, see Ritter & Kolb 2003; Brunschweiler et al. 2009) with a radius of about  $0.01 R_{\odot}$  and a shock height of the accretion column of  $\sim (1 - 2) \times 10^6 \text{ cm}$  (Yuasa et al. 2010). The hard spectrum of the source would fit in the class of IPs with hard X-ray emission (Haberl & Motch 1995), but the high absorption at lower energies could obscure an additional softer emission. The significance of the 500 s periodicity is above  $3\sigma$  in the soft  $0.5 - 2.0 \text{ keV}$  but only  $\sim 2\sigma$  in the hard  $2.0 - 10 \text{ keV}$  band. This would be expected in IPs, which usually show higher variation amplitude in the softer X-ray band (e.g. Luna et al. 2018). The residuals of the bremsstrahlung model (see Fig. 2) do not show evidence for an Fe-line complex between 6–7 keV which is often observed for IPs (e.g. Munro et al. 2004; Revnivtsev et al. 2004). The upper limits on the EW of the main Fe emission lines are consistent with previously discussed IP candidates (e.g. Hong et al. 2009). The X-ray luminosity is in the expected range, but it is among the most distant known IPs with some candidates

<sup>2</sup> <https://exoplanetarchive.ipac.caltech.edu/docs/tools.html>

<sup>3</sup> MOS2 showed a significantly more noisy background PSD (corrupting the source periodogram), compared to PN and MOS1.

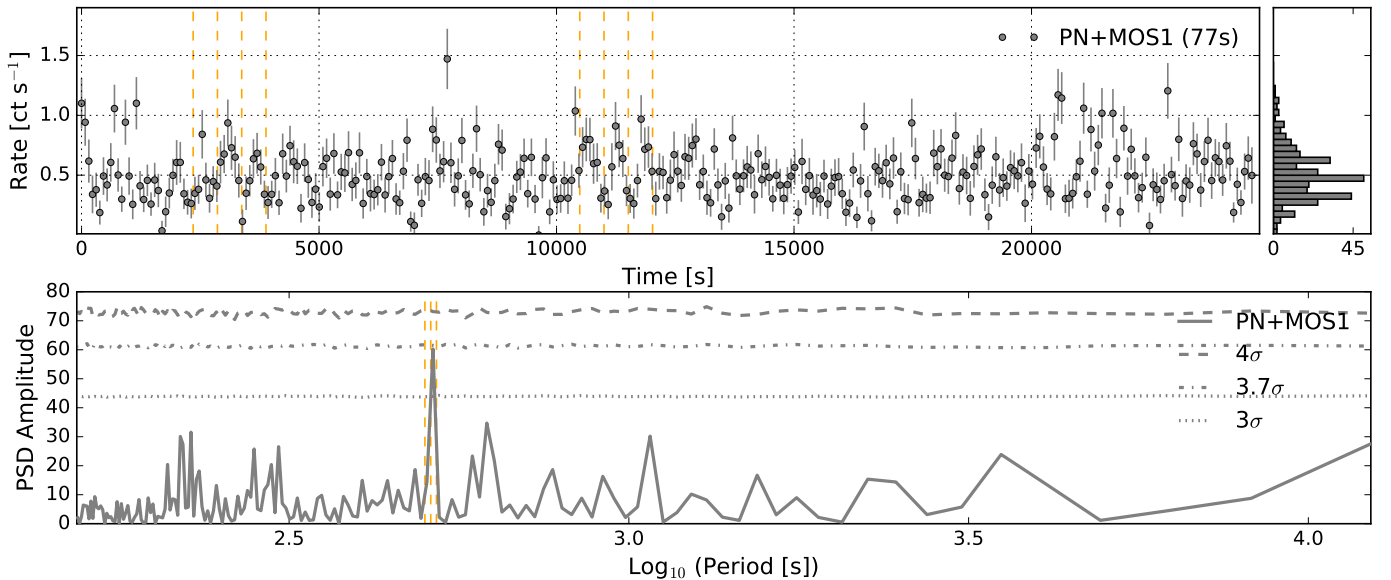


**Fig. 3. Top:** Background subtracted, vignetting corrected X-ray (0.5 – 10 keV) light curve of *XMM-Newton* EPIC PN+MOS1, binned to 77 s. Dashed orange lines mark intervals where the 511 s pulsations are visible by eye, the histogram shows the distribution of rates. **Bottom:** PSD amplitude [Rate<sup>2</sup> Hz<sup>-1</sup>]. Dashed lines show the confidence contours of simulated light curves without periodicity, assuming white noise variability. The orange dashed lines indicate the 511 ± 10 s period.

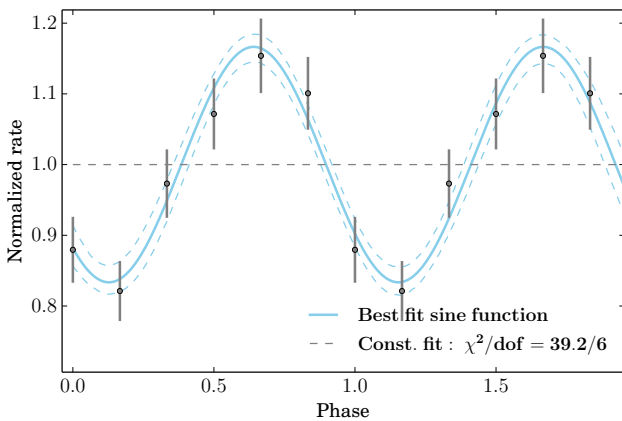


**Fig. 4.** Normalized rate over phase for the *XMM-Newton* EPIC PN light curve (77 s bins) folded by a 511 s period. The best fit sine function is displayed in blue (uncertainty from Monte Carlo simulations in dashed blue). The annotations give the goodness of fit to a constant value of 1.0 (dashed grey line).

in the GB (see e.g. Hong et al. 2009; Britt et al. 2013; Torres et al. 2014; Johnson et al. 2017) or identified from periodicity in extragalactic novae (in M 31 see e.g. Pietsch et al. 2011). The expected orbital period in the IP scenario would be  $P_{\text{orb}} \gtrsim 5000$  s ( $P_{\text{spin}}/P_{\text{orb}} \lesssim 0.1$ , Norton et al. 2004). The light curve shows a hint of modulation on time scales of  $\sim 5000$  s, but because the observation time was only 25 ks no significant detection of an orbital period was found.

#### 4.2. Source location and luminosity

The measured X-ray absorption is consistent with the expected total column density of the Galaxy ( $N_{\text{H}} = N_{\text{HI}} + 2N_{\text{H}_2} \approx 9 \times 10^{21} \text{ cm}^{-2}$ , Willingale et al. 2013) towards the source position. This provides some evidence

that the source is located close to the GC (see e.g. dust layer distribution study by Jin et al. 2017, 2018). If the source was closer (in front of the main absorbers toward the GC) it would need to have a high intrinsic absorption.

The expected X-ray luminosity range of IPs is about  $3 \times 10^{29} - 5 \times 10^{33} \text{ erg s}^{-1}$  (Ruiter et al. 2006) which constrains the distance to the source from its *XMM-Newton* flux and the *Chandra* upper limit to about 0.1 – 8 kpc. The average luminosity of the source during the *XMM-Newton* EPIC observation is  $(1.3 \pm 0.1) \times 10^{34} \text{ erg/s}$  (0.5–7.0 keV) assuming a TBabs × brems model (see Fig. 2) and a distance of 8 kpc (distance to the GC, see e.g. Eisenhauer et al. 2003). The  $3\sigma$  upper limit from previous *Chandra* observations in this case would be  $6.6 \times 10^{32} \text{ erg/s}$  (0.5–7.0 keV).

For a local IP a relatively blue optical counterpart would be expected (Hong et al. 2009) but no candidate fitting this criterion was found in the  $3\sigma$  error circle around the source position (see above). Assuming that the true counterpart is below the sensitivity limit of current catalogues ( $V_{\text{mag}} \sim 22$ ), with the typical CV magnitude range  $M_V \approx 5.5 - 10.5$  (e.g. Hong et al. 2009), and rising absorption from  $A_V \approx 1 - 4$  (estimated from Schlafly & Finkbeiner 2011; Schultheis et al. 2014) between 1 – 8 kpc, we can constrain its distance to  $\gtrsim 1$  kpc. Using the hydrogen column density measured in the X-ray spectrum, we estimate  $A_V \approx 6$  (relation by Güver & Özel 2009). If the donor star was a subdwarf like in GK Per, one of the faint optical correlations (e.g. number 1, 2, or 3 in Fig. 1) might be the true counterpart, which would be consistent with location in the GB. Hong et al. (2009) found a probable optical counterpart with  $21.7 V_{\text{mag}}$  for an IP in the GB, but located in Baade’s window where the extinction is only  $A_V \approx 1.4$  at  $\gtrsim 3$  kpc.

Together with the  $N_{\text{H}}$ , flux, and optical counterpart constraints we used the stellar density and Galactic X-ray source distribution (as shown for the GB IP candidate in Hong et al. 2009) to conclude that the new IP candidate is most likely located in the GB ( $8 \pm 2$  kpc, see overview of GB structure by Bland-Hawthorn & Gerhard 2016).

### 4.3. Alternative interpretations

Just at the border of the  $3\sigma$  positional error circle is a Be star candidate from the OGLEII survey (Sabogal et al. 2008) for which no significant variability was detected. A Be X-ray binary could show periodic pulsations similar to IPs, but the X-ray spectrum would be well fit by a powerlaw with photon index  $\approx 1$  (see e.g. the population of the Small Magellanic Cloud, Haberl & Pietsch 2004; Coe & Kirk 2015; Haberl & Sturm 2016).

From its X-ray luminosity the newly discovered source is a very faint X-ray transient (VFXT with  $L_X \approx 10^{34-36}$  erg s $^{-1}$ , see e.g. King & Wijnands 2006) and at least a factor of ten flux variation. The luminosity peaks of the source are around  $10^{34}$  erg s $^{-1}$  if it is located at GC distance. The variability within the observation does not indicate an ongoing brightening. VFXTs are still a poorly explored family of transients that are expected to be mostly X-ray binaries (neutron star or black hole as compact object) with a low accretion rate from a low-mass donor star at  $\lesssim 10^{-13}$  M $_{\odot}$ /yr (King & Wijnands 2006; Maccarone & Patruno 2013; Heinke et al. 2015).

We note that the spectrum of XMMU J175035.2-293557 is harder than for typical VFXTs (see e.g. Armas Padilla et al. 2013) and periodic pulsations are usually not observed in VFXTs. Our results show that highly variable IPs could contribute to the faint end of the VFXT population.

## 5. Conclusions

With the results of this work we constrained the nature of the newly discovered X-ray source XMMU J175035.2-293557 with the most likely scenario being an intermediate polar in the Galactic bulge. It is among the most luminous candidates, which implies a strong magnetic field of the white dwarf. The spin period of the white dwarf would be  $P_{\text{spin}} = 511 \pm 10$  s, but the orbital period of the system  $P_{\text{orb}}$  could not be recovered from the current data. The system was a factor of  $\geq 20$  fainter in observations  $\sim 10$  years before and  $\sim 6$  months after the first detection. This transient nature makes it most likely the second member of the GK Per class. The X-ray spectra are best fit by a bremsstrahlung model with a temperature of  $13.9 \pm 2.5$  keV. No optical counterpart is identified but several candidates are found. The true counterpart might be below the detection threshold of currently available surveys. With an average flux of  $\sim 1.7 \times 10^{-12}$  erg s $^{-1}$  cm $^{-2}$  this type of source will also be detected in the upcoming eROSITA all-sky survey (Merloni et al. 2012) which will allow studying a larger fraction of the Galactic population (on the order of 100 expected). Following up with high resolution and large effective area X-ray observatories like ATHENA (Nandra et al. 2013) the spin and orbital periods of similar IP systems will be significantly detected.

**Acknowledgements.** We thank the anonymous referee for very constructive comments that helped to improve the clarity of the paper. We thank M. Freyberg and C. Wegg for helpful discussions. These results are based on observations obtained with *XMM-Newton*, an ESA science mission with instruments and contributions directly funded by ESA Member States and NASA. We acknowledge the use of public data from the Swift data archive and thank the Swift team for scheduling the ToO observation; data obtained from the *Chandra* Data Archive and the *Chandra* Source Catalog, and software provided by the *Chandra* X-ray Center (CXC) in the application package CIAO; NASA's Astrophysics Data System; the VizieR catalogue access tool, CDS, Strasbourg, France; SAOImage DS9, developed by Smithsonian Astrophysical Observatory; data and/or software provided by the High Energy Astrophysics Science Archive Research Center (HEASARC), which is a service of the Astrophysics Science Division at NASA/GSFC and the High Energy Astrophysics Division of the Smithsonian Astrophysical Observatory; the SIMBAD database, operated at CDS, Strasbourg, France; NASA's SkyView facility located at NASA Goddard Space Flight Center; the NASA Exoplanet Archive, which is operated by the California Institute

of Technology, under contract with the National Aeronautics and Space Administration under the Exoplanet Exploration Program; the NASA/IPAC Infrared Science Archive, which is operated by the Jet Propulsion Laboratory, California Institute of Technology, under contract with the National Aeronautics and Space Administration; data provided by the Science Data Archive at NOAO. NOAO is operated by the Association of Universities for Research in Astronomy (AURA), Inc. under a cooperative agreement with the National Science Foundation; use of the python packages Matplotlib, scipy, numpy, and pyXSPEC. F. Hofmann and G. Ponti acknowledge financial support from the BMWi/DLR grants FKZ 50 OR 1715 and 50 OR 1604.

## References

- Armas Padilla, M., Degenaar, N., & Wijnands, R. 2013, MNRAS, 434, 1586  
 Arnaud, K. A. 1996, in Astronomical Society of the Pacific Conference Series, Vol. 101, Astronomical Data Analysis Software and Systems V, ed. G. H. Jacoby & J. Barnes, 17  
 Barbera, E., Orlando, S., & Peres, G. 2017, A&A, 600, A105  
 Bland-Hawthorn, J. & Gerhard, O. 2016, ARA&A, 54, 529  
 Britt, C. T., Torres, M. A. P., Hynes, R. I., et al. 2013, ApJ, 769, 120  
 Brunschweiler, J., Greiner, J., Ajello, M., & Osborne, J. 2009, A&A, 496, 121  
 Buchner, J., Georgakakos, A., Nandra, K., et al. 2014, A&A, 564, A125  
 Burrows, D. N., Hill, J. E., Nousek, J. A., et al. 2005, Space Sci. Rev., 120, 165  
 Calamida, A., Sahu, K. C., Anderson, J., et al. 2014, ApJ, 790, 164  
 Calamida, A., Sahu, K. C., Casertano, S., et al. 2015, ApJ, 810, 8  
 Coe, M. J. & Kirk, J. 2015, MNRAS, 452, 969  
 Cropper, M. 1990, Space Sci. Rev., 54, 195  
 Cutri, R. M., Skrutskie, M. F., van Dyk, S., et al. 2003, VizieR Online Data Catalog, 2246  
 Dobrotka, A., Mineshige, S., & Ness, J. U. 2014, MNRAS, 438, 1714  
 Downes, R. A., Webbink, R. F., Shara, M. M., et al. 2001, PASP, 113, 764  
 Eisenhauer, F., Schödel, R., Genzel, R., et al. 2003, ApJ, 597, L121  
 Fruscione, A., McDowell, J. C., Allen, G. E., et al. 2006, in Proc. SPIE, Vol. 6270, Society of Photo-Optical Instrumentation Engineers (SPIE) Conference Series, 62701V  
 Gaia Collaboration, Brown, A. G. A., Vallenari, A., et al. 2018, ArXiv e-prints [arXiv:1804.09365]  
 Garmire, G. P., Bautz, M. W., Ford, P. G., Nousek, J. A., & Ricker, Jr., G. R. 2003, in Proc. SPIE, Vol. 4851, X-Ray and Gamma-Ray Telescopes and Instruments for Astronomy., ed. J. E. Truemper & H. D. Tananbaum, 28–44  
 Girard, T. M., van Altena, W. F., Zacharias, N., et al. 2011, AJ, 142, 15  
 Graessle, D. E., Evans, I. N., Glotfelty, K., et al. 2007, Chandra News, 14, 33  
 Grindlay, J., Zhao, P., Hong, J. S., et al. 2003, Astronomische Nachrichten, 324, 57  
 Güver, T. & Özel, F. 2009, MNRAS, 400, 2050  
 Haberl, F. & Motch, C. 1995, A&A, 297, L37  
 Haberl, F. & Pietsch, W. 2004, A&A, 414, 667  
 Haberl, F. & Sturm, R. 2016, A&A, 586, A81  
 Hailey, C. J., Mori, K., Perez, K., et al. 2016, ApJ, 826, 160  
 Heinke, C. O., Bahramian, A., Degenaar, N., & Wijnands, R. 2015, MNRAS, 447, 3034  
 Hellier, C. 2007, in IAU Symposium, Vol. 243, Star-Disk Interaction in Young Stars, ed. J. Bouvier & I. Appenzeller, 325–336  
 Hellier, C. & Mukai, K. 2004, MNRAS, 352, 1037  
 Hong, J. 2012, MNRAS, 427, 1633  
 Hong, J. S., van den Berg, M., Laycock, S., Grindlay, J. E., & Zhao, P. 2009, ApJ, 699, 1053  
 Jin, C., Ponti, G., Haberl, F., & Smith, R. 2017, MNRAS, 468, 2532  
 Jin, C., Ponti, G., Haberl, F., Smith, R., & Valencic, L. 2018, ArXiv e-prints [arXiv:1802.00637]  
 Johnson, C. B., Torres, M. A. P., Hynes, R. I., et al. 2017, MNRAS, 466, 129  
 Jonker, P. G., Bassa, C. G., Nelemans, G., et al. 2011, ApJS, 194, 18  
 Jonker, P. G., Torres, M. A. P., Hynes, R. I., et al. 2014, ApJS, 210, 18  
 Kim, Y. & Beuermann, K. 1995, A&A, 298, 165  
 King, A. R. & Wijnands, R. 2006, MNRAS, 366, L31  
 Krivonos, R., Revnivtsev, M., Churazov, E., et al. 2007, A&A, 463, 957  
 Laycock, S., Grindlay, J., van den Berg, M., et al. 2005, ApJ, 634, L53  
 Luna, G. J. M., Mukai, K., Orio, M., & Zemko, P. 2018, ApJ, 852, L8  
 Maccarone, T. J. & Patruno, A. 2013, MNRAS, 428, 1335  
 Merloni, A., Predehl, P., Becker, W., et al. 2012, ArXiv e-prints [arXiv:1209.3114]  
 Minniti, D., Lucas, P., & VVV Team. 2017, VizieR Online Data Catalog, 2348  
 Mukai, K. 2017, PASP, 129, 062001  
 Muno, M. P., Arabadji, J. S., Baganoff, F. K., et al. 2004, ApJ, 613, 1179  
 Nakashima, S., Nobukawa, M., Uchida, H., et al. 2013, ApJ, 773, 20  
 Nandra, K., Barret, D., Barcons, X., et al. 2013, ArXiv e-prints [arXiv:1306.2307]  
 Norton, A. J., Wynn, G. A., & Somerscales, R. V. 2004, ApJ, 614, 349

- Osborne, J. P. 1988, *Mem. Soc. Astron. Italiana*, 59, 117
- Patterson, J. 1994, *PASP*, 106, 209
- Perez, K., Hailey, C. J., Bauer, F. E., et al. 2015, *Nature*, 520, 646
- Pietsch, W., Henze, M., Haberl, F., et al. 2011, *A&A*, 531, A22
- Ponti, G., Morris, M. R., Terrier, R., et al. 2015, *MNRAS*, 453, 172
- Pretorius, M. L. & Mukai, K. 2014, *MNRAS*, 442, 2580
- Revnivtsev, M., Lutovinov, A., Suleimanov, V., Sunyaev, R., & Zheleznyakov, V. 2004, *A&A*, 426, 253
- Revnivtsev, M., Sazonov, S., Churazov, E., et al. 2009, *Nature*, 458, 1142
- Ritter, H. & Kolb, U. 2003, *A&A*, 404, 301
- Ruiter, A. J., Belczynski, K., & Harrison, T. E. 2006, *ApJ*, 640, L167
- Sabogal, B. E., Mennickent, R. E., Pietrzyński, G., et al. 2008, *A&A*, 478, 659
- Scargle, J. D. 1982, *ApJ*, 263, 835
- Schlafly, E. F. & Finkbeiner, D. P. 2011, *ApJ*, 737, 103
- Schultheis, M., Zasowski, G., Allende Prieto, C., et al. 2014, *AJ*, 148, 24
- Shaw, A. W., Heinke, C. O., Bahramian, A., et al. 2017, in *AAS/High Energy Astrophysics Division*, Vol. 16, *AAS/High Energy Astrophysics Division*, 400.01
- Strüder, L., Briel, U., Dennerl, K., et al. 2001, *A&A*, 365, L18
- Torres, M. A. P., Jonker, P. G., Britt, C. T., et al. 2014, *MNRAS*, 440, 365
- Turner, M. J. L., Abbey, A., Arnaud, M., et al. 2001, *A&A*, 365, L27
- Udalski, A., Szymanski, M., Kubiak, M., et al. 2002, *Acta Astron.*, 52, 217
- Watson, M. G., King, A. R., & Osborne, J. 1985, *MNRAS*, 212, 917
- Wevers, T., Hodgkin, S. T., Jonker, P. G., et al. 2016, *MNRAS*, 458, 4530
- Willingale, R., Starling, R. L. C., Beardmore, A. P., Tanvir, N. R., & O’Brien, P. T. 2013, *MNRAS*, 431, 394
- Wilms, J., Allen, A., & McCray, R. 2000, *ApJ*, 542, 914
- Yuasa, T., Hayashi, T., & Ishida, M. 2016, *MNRAS*, 459, 779
- Yuasa, T., Nakazawa, K., Makishima, K., et al. 2010, *A&A*, 520, A25